한국소음진동공학회 2013년 추계학술대회논문집, pp. 206~213

두 개의 서로 다른 압전재료층 사이의 기능경사압전재료 접합층 내부 균열에 대한 과도응답 해석

Transient Response of a Crack in a Functionally Graded Piezoelectric Strip between Two Dissimilar Piezoelectric Strip

신정우† · 이영신* · 김성준**

Jeong Woo Shin, Young-Shin Lee and Sung Joon Kim

Key Words : Transient response(과도 응답), Crack(균열), Dynamic energy release rate(동에너지 해방률), Functionally graded piezoelectric material(기능경사압전재료), Interface layer(접합층)

ABSTRACT

Transient response of a crack in a functionally graded piezoelectric material (FGPM) interface layer between two dissimilar homogeneous piezoelectric layers under anti-plane shear is analyzed using integral transform approaches. The properties of the FGPM layer vary continuously along the thickness. Laplace and Fourier transforms are used to reduce the problem to two sets of dual integral equations, which are then expressed to the Fredholm integral equations of the second kind. Numerical values on the dynamic energy release rate (DERR) are presented for the FGPM to show the effects on electric loading, gradient of the material properties, and thickness of the layers. Computed results yield following conclusions: (a) the DERR increases with the increase of the gradient of the material properties of the FGPM layer; (b) certain direction and magnitude of the electric impact loading impedes crack extension; (c) increase of the thickness of the FGPM layer and the homogeneous piezoelectric layer which has larger material properties than those of the crack plane are beneficial to increase of the resistance of transient fracture of the FGPM layer.

본 논문에서는 적분변환법을 이용하여 면외전단 충격하중이 작용하는 두 개의 서로 다른 압전재료층 사이의 기능경사압전재료 접합층 내부 균열에 대한 과도응답 해석을 수행한다. 기능경사압전재료의 물성치는 두께 방향을 따라 연속적으로 변하는 것으로 가정한다. 라플라스 변환과 푸리에 변환을 이용하여 문제를 복합적분방정식으로 구성하고, 수치해석을 위해 복합적분방정식을 제 2 종 프레드홀름 적분방정식으로 표현한다. 전기적 하중, 재료물성치의 변화율, 각 접합층의 두께가 균열의 과도응답에 미치는 영향을 보기 위해 동에너지 해방률에 대한 수치해석 결과를 제시한다.

1. Introduction

Owing to their intrinsic electromechanical coupling effects, piezoelectric materials have been widely used in smart sensors, transducers and actuators. In practical usage, bonding of dissimilar piezoelectric layers is frequently happened. However, the interface plane of the bonding structure is susceptible to developing cracks because of mismatch of material properties. Fracture analysis of functionally graded piezoelectric materials (FGPMs) as an interface layer has been attracted extensive attention in order to solve the mismatch of material properties. The FGPMs are microscopically non-homogeneous because the mechanical properties of the FGPM vary continuously. A

† 교신저자 ; 한국항공우주연구원 항공구조팀
E-mail : jeongdal@kari.re.kr
Tel : 042-860-2026, Fax : 042-860-2604
* 충남대학교 기계설계공학과
** 한국항공우주연구원 항공구조팀

crack in the FGPM may exhibit complex behavior because of the variation of the mechanical properties of the material. Significant efforts have been made in the study of the FGPMs.

A few researches concerned with the transient response of crack in FGPMs were reported[1~4]. And much fewer studies have been conducted for the interface crack problem of the FGPMs[5~10]. Recently, Yan and Jiang[11] and Shin and Lee[12] studied moving crack in a FGPM interface layer between two homogeneous piezoelectric bodies. But, solution of transient response of a crack in a FGPM interface layer between two dissimilar piezoelectric layers has not been presented.

In this paper, transient response of a Griffith crack in a FGPM interface layer between two dissimilar homogeneous piezoelectric layers under anti-plane shear is analyzed. The properties of a FGPM layer vary continuously along the thickness. The FGPM layer and two piezoelectric layers are connected weak-discontinuously[13]. Laplace and Fourier transforms are used to reduce the problem to two sets of dual integral equations, which are then expressed in two Fredholm integral equations of the second kind. Numerical results of the dynamic energy release (DERR) are presented graphically to show the effects on electric loading, gradient of material properties, and thickness of layers.

2. Problem statement and formulation

Consider a FGPM interface layer containing a finite eccentric crack sandwiched between two homogeneous piezoelectric layers, which is subjected to the combined mechanical and electrical Heaviside step pulse loadings as shown in Fig. 1. The Cartesian coordinates (x, y, z) are attached to the center of the crack. The FGPM and homogeneous piezoelectric layers are poled with z-axis, and are thick enough in the z-direction to allow a state of anti-plane shear. The FGPM layer occupies the region, $-\infty < x < \infty$, $-h_2 \le y \le h_1$, $2h = h_1 + h_2$. For convenience, we assume that the upper ($y \ge 0$, thickness h_1) and lower ($y \le 0$, thickness h_2) regions of the FGPM layer cracked have different thickness but consist the same FGPMs. The crack is situated along the virtual interface line ($-a \le x \le a,\ y = 0$). Due to the symmetry in geometry and loading, it is sufficient to consider the right-hand half body only.

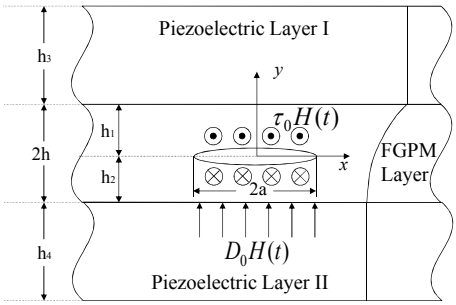

Fig. 1 Definition of geometry and loading

We assume that the properties of the FGPM layer vary smoothly and continuously along the thickness and are simplified as follows[14]:

$$c_{44} = c_{440}\exp(\beta y),\ d_{11} = d_{110}\exp(\beta y),\ e_{15} = e_{150}\exp(\beta y),\ \rho = \rho_0\exp(\beta y) \quad (1)$$

where c_{44}, d_{11}, e_{15} and ρ are the elastic modulus, dielectric permittivity, piezoelectric constant and material density, respectively. c_{440}, d_{110}, e_{150} and ρ_0 are the material properties at $y = 0$ and β is the non-homogeneous material constant. The material properties are the same values at $y = h_1$ and $y = -h_2$ for the FGPM layer and the homogeneous piezoelectric layers.

The piezoelectric boundary value problem is simplified considerably if we consider only the out-of-plane displacement and the in-plane electric fields such that

$$u_{xi}^F = u_{yi}^F = 0,\ u_{zi}^F = w_i^F(x,y,t) \quad (2)$$

$$E_{xi}^F = E_{xi}^F(x,y,t),\ E_{yi}^F = E_{yi}^F(x,y,t),\ E_{zi}^F = 0 \quad (3)$$

$$u_{xi}^H = u_{yi}^H = 0,\ u_{zi}^H = w_i^H(x,y,t) \quad (4)$$

$$E_{xi}^H = E_{xi}^H(x,y,t),\ E_{yi}^H = E_{yi}^H(x,y,t),\ E_{zi}^H = 0 \quad (5)$$

where u_{ki} and E_{ki} ($k = x, y, z$) are the displacements and electric fields, respectively. Superscripts F and H stand for a FGPM layer and the homogeneous piezoelectric layers, respectively. And subscript $i (i = 1, 2)$ stands for upper and lower regions, respectively, for both FGPM layer and homogeneous piezoelectric layers.

In this case, the constitutive relations become

$$\sigma_{Zji}^F(x,y,t) = c_{44}w_{i,j}^F + e_{15}\phi_{i,j}^F \quad (6)$$

$$D_{ji}^{F}(x,y,t) = e_{15} w_{i,j}^{F} - d_{11} \phi_{i,j}^{F} \tag{7}$$

$$\sigma_{Zji}^{H}(x,y,t) = c_{44i} w_{i,j}^{H} + e_{15i} \phi_{i,j}^{H} \tag{8}$$

$$D_{ji}^{H}(x,y,t) = e_{15i} w_{i,j}^{H} - d_{11i} \phi_{i,j}^{H} \tag{9}$$

where σ_{zji}, D_{ji}, ($j = x, y$) and ϕ_i are the stress components, electric displacements and electric potential, respectively. c_{44i}, d_{11i}, e_{15i} and ρ_i are the material properties for the homogeneous piezoelectric layers.

The dynamic anti-plane governing equations for FGPM and homogeneous piezoelectric material are simplified to

$$\begin{aligned} & c_{44} \nabla^2 w_i^F + e_{15} \nabla^2 \phi_i^F \\ & + \beta (c_{44} \frac{\partial w_i^F}{\partial y} + e_{15} \frac{\partial \phi_i^F}{\partial y}) = \rho \frac{\partial^2 w_i^F}{\partial t^2} \end{aligned} \tag{10}$$

$$\begin{aligned} & e_{15} \nabla^2 w_i^F - d_{11} \nabla^2 \phi_i^F \\ & + \beta (e_{15} \frac{\partial w_i^F}{\partial y} - d_{11} \frac{\partial \phi_i^F}{\partial y}) = 0 \end{aligned} \tag{11}$$

$$c_{44i} \nabla^2 w_i^H + e_{15i} \nabla^2 \phi_i^H = \rho_i \frac{\partial^2 w_i^H}{\partial t^2} \tag{12}$$

$$e_{15i} \nabla^2 w_i^H - d_{11i} \nabla^2 \phi_i^H = 0 \tag{13}$$

where $\nabla^2 = \partial^2 / \partial x^2 + \partial^2 / \partial y^2$.

The Laplace transforms of Eqs. (10) ~ (13) are the followings:

$$\nabla^2 w_i^{F*} + \beta \frac{\partial w_i^{F*}}{\partial y} = \frac{p^2}{c_2^2} w_i^{F*} \tag{14}$$

$$\nabla^2 \psi_i^{F*} + \beta \frac{\partial \psi_i^{F*}}{\partial y} = 0 \tag{15}$$

$$\nabla^2 w_i^{H*} = \frac{p^2}{c_2^2} w_i^{H*} \tag{16}$$

$$\nabla^2 \psi_i^{H*} = 0 \tag{17}$$

where

$$w_i^*(x,y,p) = \int_0^\infty w_i(x,y,t) \exp(-pt) dt \tag{18}$$

$$w_i(x,y,t) = \frac{1}{2\pi i} \int_{c-i\infty}^{c+i\infty} w_i^*(x,y,p) \exp(pt) dp \tag{19}$$

$$\phi_i^*(x,y,p) = \int_0^\infty \phi_i(x,y,t) \exp(-pt) dt \tag{20}$$

$$\phi_i(x,y,t) = \frac{1}{2\pi i} \int_{c-i\infty}^{c+i\infty} \phi_i^*(x,y,p) \exp(pt) dp \tag{21}$$

$$\psi_i^* = \phi_i^* - \frac{e_{150}}{d_{110}} w_i^* \tag{22}$$

$$c_2 = \sqrt{\mu_0 / \rho_0} \ , \ \ \mu_0 = c_{440} + {e_{150}}^2 / d_{110} \tag{23}$$

and c_2 is the shear wave velocity and μ_0 is piezoelectrically stiffened elastic constant at the crack plane. The superscript * stands for the Laplace transform domain.

Fourier transforms are applied to Eqs. (14) ~ (17), and the results are as follows:

$$w_i^{F*}(x,y,p) = \frac{2}{\pi} \int_0^\infty \begin{bmatrix} A_{1i}(s,p) \exp(-q_1 y) \\ + A_{2i}(s,p) \exp(q_2 y) \end{bmatrix} \cos(sx) ds \tag{24}$$

$$\begin{aligned} \phi_i^{F*}(x,y,p) = & \frac{2}{\pi} \frac{e_{150}}{d_{110}} \int_0^\infty \begin{bmatrix} A_{1i}(s,p) \exp(-q_1 y) \\ + A_{2i}(s,p) \exp(q_2 y) \end{bmatrix} \cos(sx) ds \\ & + \frac{2}{\pi} \int_0^\infty \begin{bmatrix} B_{1i}(s,p) \exp(-p_1 y) \\ + B_{2i}(s,p) \exp(p_2 y) \end{bmatrix} \cos(sx) ds \end{aligned} \tag{25}$$

$$w_i^{H*}(x,y,p) = \frac{2}{\pi} \int_0^\infty \begin{bmatrix} A_{3i}(s,p) \exp(-\gamma y) \\ + A_{4i}(s,p) \exp(\gamma y) \end{bmatrix} \cos(sx) ds \tag{26}$$

$$\begin{aligned} \phi_i^{H*}(x,y,p) = & \frac{2}{\pi} \frac{e_{150}}{d_{110}} \int_0^\infty \begin{bmatrix} A_{3i}(s,p) \exp(-\gamma y) \\ + A_{4i}(s,p) \exp(\gamma y)) \end{bmatrix} \cos(sx) ds \\ & + \frac{2}{\pi} \int_0^\infty \begin{bmatrix} B_{3i}(s) \exp(-sy) \\ + B_{4i}(s) \exp(sy) \end{bmatrix} \cos(sx) ds \end{aligned} \tag{27}$$

where

$$\begin{aligned} & q_1 = \delta + \beta/2 \ , \ \ q_2 = \delta - \beta/2 \ , \\ & p_1 = \lambda + \beta/2 \ , \ \ p_2 = \lambda - \beta/2 \end{aligned} \tag{28}$$

$$\delta = \sqrt{\gamma^2 + \beta^2/4} \ , \ \ \lambda = \sqrt{s^2 + \beta^2/4} \tag{29}$$

$$\gamma = \sqrt{s^2 + p^2 / c_2^2} \tag{30}$$

A_{1i}, A_{2i}, A_{3i}, A_{4i}, B_{1i}, B_{2i}, B_{3i} and B_{4i} are the unknowns to be solved.

In this case, the stress and electric displacement components are as follows:

$$\begin{aligned} \sigma_{yzi}^{F*}(x,y,p) = & \ \mu_0 \frac{2}{\pi} \int_0^\infty \begin{bmatrix} -q_1 A_{1i}(s,p) \exp(-q_2 y) \\ + q_2 A_{2i}(s,p) \exp(q_1 y) \end{bmatrix} \cos(sx) ds \\ & + e_{150} \frac{2}{\pi} \int_0^\infty \begin{bmatrix} -p_1 B_{1i}(s,p) \exp(-p_2 y) \\ + p_2 B_{2i}(s) \exp(p_1 y) \end{bmatrix} \cos(sx) ds \end{aligned} \tag{31}$$

$$D_{yi}^{F*}(x,y,p) = -d_{110} \frac{2}{\pi} \int_0^\infty \begin{bmatrix} -p_1 B_{1i}(s,p) \exp(-p_2 y) \\ + p_2 B_{2i}(s,p) \exp(p_1 y) \end{bmatrix} \cos(sx) ds \tag{32}$$

$$\begin{aligned} \sigma_{yzi}^{H*}(x,y,p) = & \ \mu_i \frac{2}{\pi} \int_0^\infty \begin{bmatrix} -\gamma A_{3i}(s,p) \exp(-\gamma y) \\ + \gamma A_{4i}(s,p) \exp(\gamma y) \end{bmatrix} \cos(sx) ds \\ & + e_{15i} \frac{2}{\pi} \int_0^\infty \begin{bmatrix} -s B_{3i}(s,p) \exp(-sy) \\ + s B_{4i}(s,p) \exp(sy) \end{bmatrix} \cos(sx) ds \end{aligned} \tag{33}$$

$$D_{yi}^{H^*}(x,y,p) = -d_{11i}\frac{2}{\pi}\int_0^{\infty}\begin{bmatrix}-sB_{3i}(s,p)\exp(-sy)\\+sB_{4i}(s,p)\exp(sy)\end{bmatrix}\cos(sx)ds \quad (34)$$

where

$$\mu_i = c_{44i} + {e_{15i}}^2 \big/ d_{11i} \ . \quad (35)$$

The mixed boundary conditions can be written as

$$\sigma_{yzi}^{F*}(x,0,p) = -\tau_0 / p\,, \qquad (0 \le x < a) \quad (36)$$

$$w_1^{F*}(x,0^+,p) = w_2^{F*}(x,0^-,p)\,, \qquad (a < x \le \infty) \quad (37)$$

$$D_{yi}^{F*}(x,0,p) = -D_0 / p\,, \qquad (0 \le x < a) \quad (38)$$

$$\phi_1^{F*}(x,0^+,p) = \phi_1^{F*}(x,0^-,p)\,, \qquad (a < x \le \infty) \quad (39)$$

where τ_0 and D_0 are the uniform shear traction and electric displacement, respectively.

It is convenient to use the following definitions:

$$A_{11}(s,p) - A_{12}(s,p) + A_{21}(s,p) - A_{22}(s,p) = A(s,p) \quad (40)$$

$$B_{11}(s,p) - B_{12}(s,p) + B_{21}(s,p) - B_{22}(s,p) = B(s,p)\,. \quad (41)$$

The two mixed boundary conditions of Eqs. (36) to (39) lead to two sets of dual integral equation in the following forms:

$$\int_0^{\infty} s\frac{2}{s}\frac{L_1(s,p)}{L_2(s,p)}A(s,p)\cos(sx)ds = \frac{\pi}{2}\frac{2}{p}\frac{1}{\mu_0}\left(\tau_0 + \frac{e_{150}}{d_{110}}D_0\right), \quad (0 \le x < a),$$

$$\int_0^{\infty} A(s,p)\cos(sx)ds = 0\,, \qquad (a < x \le \infty) \quad (42)$$

$$\int_0^{\infty} s\frac{2}{s}\frac{M_1(s)}{M_2(s)}B(s,p)\cos(sx)ds = -\frac{\pi}{2}\frac{2}{p}\frac{D_0}{d_{110}}, \quad (0 \le x < a),$$

$$\int_0^{\infty} B(s,p)\cos(sx)ds = 0\,, \qquad (a < x \le \infty) \quad (43)$$

where

$$\begin{aligned} L_1(s,p) = {} & [q_1\{C_{11}(s,p) + \eta C_{21}(s,p)\} \\ & - q_2\exp(-2\delta h_1)\{kC_{11}(s,p) + \eta C_{21}(s,p)\}] \\ & \times[k\exp(-2\gamma h_2)(1-\exp(-2\delta h_2))D_{11}(s,p) \\ & + \eta(1 - k\exp(-2\delta h_2))D_{21}(s,p)] \end{aligned} \quad (44)$$

$$\begin{aligned} L_2(s,p) = {} & (1+k)[k\exp(-2\gamma h_2)C_{11}(s,p)D_{11}(s,p)(1-\exp(-4\delta h)) \\ & + \eta C_{11}(s,p)D_{21}(s,p)(1 - k\exp(-4\delta h)) \\ & + \eta\exp(-2\gamma h_2)C_{21}(s,p)D_{11}(s,p)(k - \exp(-4\delta h)) \\ & + \eta^2 C_{21}(s,p)D_{21}(s,p)(1 - \exp(-4\delta h))] \end{aligned} \quad (45)$$

$$\begin{aligned} M_1(s) = {} & [p_1\{C_{12}(s) + \varsigma C_{22}(s)\} \\ & - p_2\exp(-2\lambda h_1)\{fC_{12}(s) + \varsigma C_{22}(s)\}] \\ & \times[f\exp(-2sh_2)(1-\exp(-2\lambda h_2))D_{12}(s) \\ & + \varsigma(1 - f\exp(-2\lambda h_2))D_{22}(s)] \end{aligned} \quad (46)$$

$$\begin{aligned} M_2(s) = {} & (1+f)[f\exp(-2sh_2)C_{12}(s)D_{12}(s)(1-\exp(-4\lambda h)) \\ & + \varsigma C_{12}(s)D_{22}(s)(1 - f\exp(-4\lambda h)) \\ & + \varsigma\exp(-2sh_2)C_{22}(s)D_{12}(s)(f - \exp(-4\lambda h)) \\ & + \varsigma^2 C_{22}(s)D_{22}(s)(1-\exp(-4\lambda h))] \end{aligned} \quad (47)$$

$$k = q_1/q_2\,, \quad f = p_1/p_2\,, \quad \eta = \gamma/q_2\,, \quad \varsigma = s/p_2 \quad (48)$$

$$C_{11}(s,p) = 1 + \exp(-2\gamma h_3)\,, \quad C_{21}(s,p) = 1 - \exp(-2\gamma h_3)\,,$$
$$D_{11}(s,p) = 1 + \exp(-2\gamma h_4)\,, \quad D_{21}(s,p) = 1 - \exp(-2\gamma h_4) \quad (49)$$

$$C_{12}(s) = 1 + \exp(-2sh_3)\,, \quad C_{22}(s) = 1 - \exp(-2sh_3)\,,$$
$$D_{12}(s) = 1 + \exp(-2sh_4)\,, \quad D_{22}(s) = 1 - \exp(-2sh_4)\,. \quad (50)$$

To solve the two sets of dual integral equation of Eqs. (42) and (43), we define $A(s,p)$ and $B(s,p)$ in the forms,

$$A(s,p) = \frac{\pi}{2}\frac{2}{p}\frac{a^2}{\mu_0}\left(\tau_0 + \frac{e_{150}}{d_{110}}D_0\right)\int_0^1\sqrt{\Xi}\,\Psi_1^*(\Xi,p)J_0(as\Xi)d\Xi\,,$$

$$B(s,p) = -\frac{\pi}{2}\frac{2}{p}\frac{a^2 D_0}{d_{110}}\int_0^1\sqrt{\Xi}\,\Psi_2^*(\Xi)J_0(as\Xi)d\Xi \quad (51)$$

where J_0 is the zero-order Bessel function of the first kind.

By inserting Eq. (51) into Eqs. (42) and (43), we can find that the auxiliary functions $\Psi_1^*(\Xi,p)$ and $\Psi_2^*(\Xi)$ are given by the Fredholm integral equations of the second kind in the following forms:

$$\Psi_1^*(\Xi,p) + \int_0^1 N_1(\Xi,\mathrm{H},p)\Psi_1^*(\mathrm{H},p)d\mathrm{H} = \sqrt{\Xi} \quad (52)$$

$$\Psi_2^*(\Xi) + \int_0^1 N_2(\Xi,\mathrm{H})\Psi_2^*(\mathrm{H})d\mathrm{H} = \sqrt{\Xi} \quad (53)$$

where

$$N_1(\Xi,\mathrm{H},p) = \sqrt{\Xi\mathrm{H}}\int_0^{\infty} S\left[\frac{2}{S}\frac{L_1(S/a,p)}{L_2(S/a,p)} - 1\right]J_0(S\mathrm{H})J_0(S\Xi)dS \quad (54)$$

$$N_2(\Xi,\mathrm{H}) = \sqrt{\Xi\mathrm{H}}\int_0^{\infty} S\left[\frac{2}{S}\frac{M_1(S/a)}{M_2(S/a)} - 1\right]J_0(S\mathrm{H})J_0(S\Xi)dS \quad (55)$$

$$L_1(\frac{S}{a},p)=[Q_1\{C_{11}(\frac{S}{a},p)+\eta C_{21}(\frac{S}{a},p)\}$$
$$-Q_2\exp(-2\Delta\frac{h_1}{a})\{kC_{11}(\frac{S}{a},p)+\eta C_{21}(\frac{S}{a},p)\}]$$
$$\times[k\exp(-2\Gamma\frac{h_2}{a})(1-\exp(-2\Delta\frac{h_2}{a}))D_{11}(\frac{S}{a},p)$$
$$+\eta(1-k\exp(-2\Delta\frac{h_2}{a}))D_{21}(\frac{S}{a},p)] \quad (56)$$

$$L_2(\frac{S}{a},p)=(1+k)[k\exp(-2\Gamma\frac{h_2}{a})C_{11}(\frac{S}{a},p)D_{11}(\frac{S}{a},p)(1-\exp(-4\Delta\frac{h}{a}))$$
$$+\eta C_{11}(\frac{S}{a},p)D_{21}(\frac{S}{a},p)(1-k\exp(-4\Delta\frac{h}{a}))$$
$$+\eta\exp(-2\Gamma\frac{h_2}{a})C_{21}(\frac{S}{a},p)D_{11}(\frac{S}{a},p)(k-\exp(-4\Delta\frac{h}{a})) \quad (57)$$
$$+\eta^2C_{21}(\frac{S}{a},p)D_{21}(\frac{S}{a},p)(1-\exp(-4\Delta\frac{h}{a}))]$$

$$M_1(\frac{S}{a})=[P_1\{C_{12}(\frac{S}{a})+\varsigma C_{22}(\frac{S}{a})\}$$
$$-P_2\exp(-2\Lambda\frac{h_1}{a})\{fC_{12}(\frac{S}{a})+\varsigma C_{22}(\frac{S}{a})\}]$$
$$\times[f\exp(-2S\frac{h_2}{a})(1-\exp(-2\Lambda\frac{h_2}{a}))D_{12}(\frac{S}{a}) \quad (58)$$
$$+\varsigma(1-f\exp(-2\Lambda\frac{h_2}{a}))D_{22}(\frac{S}{a})]$$

$$M_2(\frac{S}{a})=(1+f)[f\exp(-2S\frac{h_2}{a})C_{12}(\frac{S}{a})D_{12}(\frac{S}{a})(1-\exp(-4\Lambda\frac{h}{a}))$$
$$+\varsigma C_{12}(\frac{S}{a})D_{22}(\frac{S}{a})(1-f\exp(-4\Lambda\frac{h}{a})) \quad (59)$$
$$+\varsigma\exp(-2S\frac{h_2}{a})C_{22}(\frac{S}{a})D_{12}(\frac{S}{a})(f-\exp(-4\Lambda\frac{h}{a}))$$
$$+\varsigma^2C_{22}(\frac{S}{a})D_{22}(\frac{S}{a})(1-\exp(-4\Lambda\frac{h}{a}))]$$

$$C_{11}(\frac{S}{a},p)=1+\exp(-2\Gamma\frac{h_3}{a}),\quad C_{21}(\frac{S}{a},p)=1-\exp(-2\Gamma\frac{h_3}{a}),$$
$$D_{11}(\frac{S}{a},p)=1+\exp(-2\Gamma\frac{h_4}{a}),\quad D_{21}(\frac{S}{a},p)=1-\exp(-2\Gamma\frac{h_4}{a}) \quad (60)$$

$$C_{12}(\frac{S}{a})=1+\exp(-2S\frac{h_3}{a}),\quad C_{22}(\frac{S}{a})=1-\exp(-2S\frac{h_3}{a}),$$
$$D_{12}(\frac{S}{a})=1+\exp(-2S\frac{h_4}{a}),\quad D_{22}(\frac{S}{a})=1-\exp(-2S\frac{h_4}{a}) \quad (61)$$

$$\Delta=\sqrt{\Gamma^2+\mathrm{B}^2/4},\quad \Lambda=\sqrt{S^2+\mathrm{B}^2/4},$$
$$\Gamma=\sqrt{S^2+p^2/(c_2/a)^2} \quad (62)$$

$$Q_1=\Delta+\mathrm{B}/2,\quad Q_2=\Delta-\mathrm{B}/2,$$
$$P_1=\Lambda+\mathrm{B}/2,\quad P_2=\Lambda-\mathrm{B}/2 \quad (63)$$

$$k=Q_1/Q_2,\quad f=P_1/P_2,\quad \eta=\Gamma/Q_2,\quad \varsigma=S/P_2 \quad (64)$$

$$S=as,\quad \mathrm{B}=a\beta. \quad (65)$$

By evaluating the dynamic energy release rate $G_{III}(t)$ for the anti-plane case obtained by Pak[15] on a vanishingly small contour at a crack tip, we can obtain the following form:

$$G_{III}(t)=\frac{K^{\tau}(t)K^{\gamma}(t)-K^{D}(t)K^{E}(t)}{2}$$
$$=\frac{\pi a}{2}\left\{\left(\tau_0+\frac{e_{150}}{d_{110}}D_0\right)^2\frac{1}{\mu_0}\left(M(t)\right)^2-\frac{{D_0}^2}{d_{110}}\left(\Psi_2^*(1)\right)^2\right\} \quad (66)$$

where

$$M(t)=\frac{1}{2\pi i}\int_{c-i\infty}^{c+i\infty}\frac{\Psi_1^*(1,p)}{p}\exp(pt)dp \quad (67)$$

in which the functions $\Psi_1^*(1,p)$ and $\Psi_2^*(1)$ can be calculated from Eqs. (52) and (53).

3. Discussions

To investigate the effects on the electric loading, gradient of the material properties and thickness of layers on the DERR, numerical analyses are carried out. The DERR is normalized by $G_\infty=\pi a{\tau_0}^2/(2\mu_0)$. The normalized electric displacement is determined as $ND_0=e_{150}D_0/(d_{110}\tau_0)$. It is assumed that the material properties at $y=0$ are the same as those of PZT-5H as follows[16]:

$$c_{440}=2.3\times10^{10}\ N/m^2,\ e_{150}=17.0\ C/m^2,$$
$$d_{110}=150.4\times10^{-10}\ C/Vm$$

From Figs. 2 to 7, a general feature of the curves is observed. The DERR rises rapidly with time, reaching a peak then decreases in magnitude to reaches its static value.

Fig. 2 presents variation of the normalized DERR $G_{III}(t)/G_\infty$ against the normalized time c_2t/a with the various normalized non-homogeneous material constant of the FGPM layer. The Peak value of DERR increases and the DERR rises more rapidly with time when the gradient of material properties of the FGPM interface layer increases. Also the peak value of DERR of the FGPM interface layer is higher than that of homogeneous piezoelectric material ($\mathrm{B}=0$). Though the DERR in the FGPM is increased, this deleterious effect is completely offset by the high fracture toughness of the FGPM, and as a result, the residual strength of the cracked FGPM is much higher than that of the homogeneous piezoelectric ceramic[17].

Fig. 3 displays variation of the normalized DERR

$G_{III}(t)/G_\infty$ against the normalized time $c_2 t/a$ with the various normalized electric displacement ND_0. The peak value of DERR increases or decreases and the DERR rises rapidly or slowly with time depending on direction and magnitude of the electric impact loading. And the sign of DERR is negative for certain electric impact load. That means the certain electric impact loading impedes crack extension. In addition, the normalized DERRs are same for the same definite electric impact loadings at $c_2 t/a = 0$. These results agree with those of researches adopted the impermeable crack boundary condition [18~20].

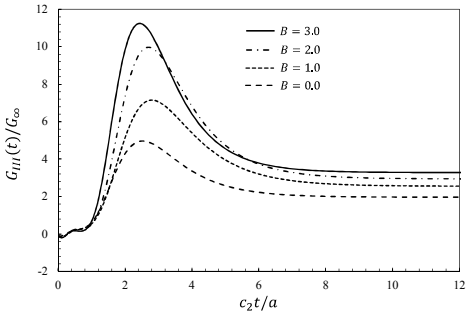

Fig. 2 Variation of the normalized DERR $G_{III}(t)/G_\infty$ with $c_2 t/a$ for various B

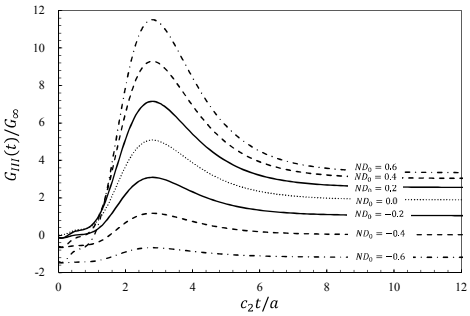

Fig. 3 Variation of the normalized DERR $G_{III}(t)/G_\infty$ with $c_2 t/a$ for various ND_0

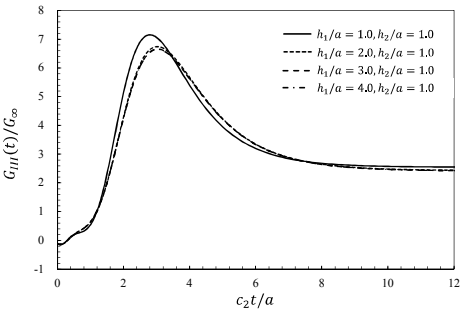

Fig. 4 Variation of the normalized DERR $G_{III}(t)/G_\infty$ with $c_2 t/a$ for various h_1/a

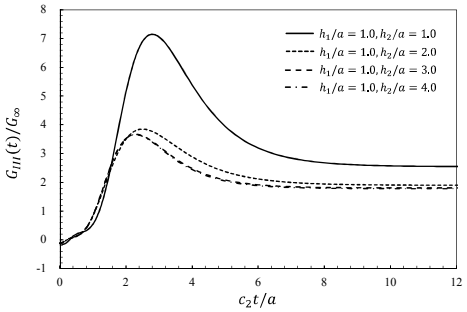

Fig. 5 Variation of the normalized DERR $G_{III}(t)/G_\infty$ with $c_2 t/a$ for various h_2/a

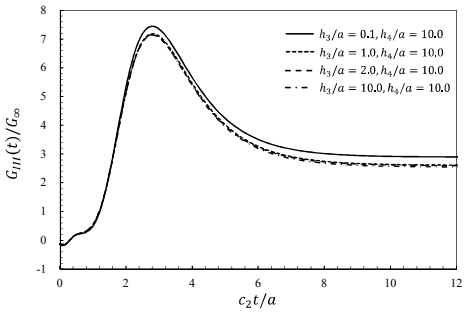

Fig. 6 Variation of the normalized DERR $G_{III}(t)/G_\infty$ with $c_2 t/a$ for various h_3/a

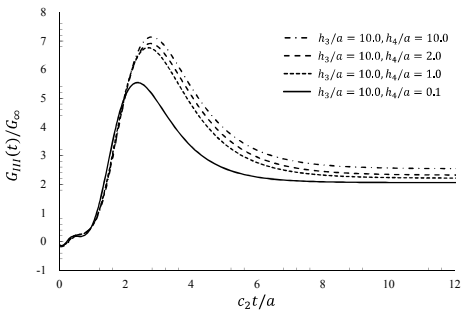

Fig. 7 Variation of the normalized DERR $G_{III}(t)/G_\infty$ with $c_2 t/a$ for various h_4/a

Fig. 4 and Fig. 5 show variation of the normalized DERR $G_{III}(t)/G_\infty$ against the normalized time $c_2 t/a$ with the various normalized thickness of the FGPM interface layer. The peak value of DERR decreases with the increase of the thickness of the FGPM interface layer. In the other word, increase of the FGPM interface layer is helpful to increase of the resistance of transient fracture of the FGPM interface layer.

Fig. 6 and Fig. 7 show variation of the normalized DERR $G_{III}(t)/G_\infty$ against the normalized time $c_2 t/a$ with the various normalized thickness of the homogeneous

piezoelectric layers. The peak value of DERR decreases with the increase of the thickness of the upper homogeneous piezoelectric layer (h_3 / a). On the contrary, the peak value of DERR increases with the increase of the thickness of the lower homogeneous piezoelectric layer (h_4 / a). Material properties of the upper homogeneous piezoelectric layer are bigger than those of the crack plane, but material properties of the lower homogeneous piezoelectric layer are less than those of the crack plane. That is, increase of the thickness of the layer which has larger material properties than those of the crack plane is beneficial to increase of the resistance of transient fracture of the FGPM interface layer.

From Fig. 4~Fig. 7, variations of the peak value of the DERR are not sensitive to the variations of the thickness of the layers which have bigger material properties than those of the crack plane (h_1 / a and h_3 / a). But variations of peak value of the DERR are sensitive to variations of the thickness of the layers which have smaller material properties than those of the crack plane (h_2 / a and h_4 / a). However, over certain value of the normalized thickness of the layers (about 3.00), the effect of variation of the peak value of the DERR is negligible.

4. Conclusions

The problem of transient response of a crack in a FGPM interface layer between two dissimilar homogeneous piezoelectric layers under anti-plane shear loading was analyzed by the integral transform approach. The material properties of the FGPM interface layer vary continuously along the thickness. The Fredholm integral equations were solved numerically. The following conclusions can be made:

- Peak value of the DERR increases and the DERR rises more rapidly with time as the gradient of the material properties of the FGPM interface layer increases
- Peak value of the DERR increases or decreases and the DERR rises rapidly or slowly with time depending on direction and magnitude of the electric impact loading. Certain direction and magnitude of the electric impact loading impedes crack extension
- Increase of the thickness of the FGPM interface layer and the homogeneous piezoelectric layer which has larger material properties than those of the crack plane are helpful to increase of the resistance of transient fracture of the FGPM interface layer. Over certain thickness of the layers, thickness effect on the DERR is negligible.

후 기

This study was supported by the ‘Research on Core Technology for Electrically Powered HALE UAVs’ program funded by the Korea Research Council of Fundamental Science & Technology, Republic of Korea.

참 고 문 헌

(1) Chen, J., Liu, Z.X. and Zou, Z.Z., 2003, The central crack problem for a functionally graded piezoelectric strip, Int. J. Fract. Vol. 121, pp. 81~94.

(2) Shin, J.W., Kim, T.U. and Kim, S.C., 2004, Dynamic characteristics of an eccentric crack in a functionally graded piezoelectric ceramic strip, J. Mech. Sci. Technol. Vol. 18, pp. 1582~1589.

(3) Sun, J.L., Zhou, Z.G. and Wang, B., 2005, Dynamic behavior of a crack in a functionally graded piezoelectric strip bonded to two dissimilar half piezoelectric material planes, Acta. Mech. Vol. 176, pp. 45~60.

(4) Ueda, S., 2007, Electromechanical impact of an impermeable parallel crack in a FGPM strip, Euro. J. Mech. A/Solids. Vol. 26, pp. 123~136.

(5) Li, Y.D. and Lee, K.Y., 2009, Anti-plane fracture analysis for the weak-discontinuous interface in a non-homogeneous piezoelectric bi-material structure, Euro. J. Mech. A/Solids. Vol. 28, pp. 241~247.

(6) Li, Y.D. and Lee, K.Y., 2010, Interfacial fracture analysis of a graded piezoelectric layer on a substrate with finite dimension, Arch. Appl. Mech. Vol. 80, pp. 1007~-1016.

(7) Shin, J.W. and Lee, Y.-S., 2011, Dynamic propagation of a weak-discontinuous interface crack between two dissimilar functionally graded layers under anti-plane shear, J. Mech. Sci. Technol. Vol. 25, pp. 2551~2557.

(8) Shin, J.W. and Lee, Y.-S., 2010, A moving interface crack between two dissimilar functionally graded piezoelectric layers under electromechanical

loading, Int. J. Solids Strut. Vol. 47, pp. 2706~2713.

(9) Ing, Y.S. and Chen, J.H., 2013, Dynamic fracture analysis of an interface crack in a two-layered functionally graded piezoelectric strip, Theor. Appl. Fract. Mech. Vol. 63~64, pp. 40-49.

(10) Shin, J.W., Lee, Y.-S. and Kim, S.J., 2013, An interface crack in a functionally graded piezoelectric bi-layer under anti-plane shear impact, Acta Mech. Vol. 224, pp. 867~879.

(11) Yan, Z. and Jiang, L.Y., 2009, On a moving dielectric crack in a piezoelectric interface with spatially varying properties, Eng. Fract. Mech. Vol. 76, pp. 560~579.

(12) Shin, J.W. and Lee, Y.-S., 2012, Anti-plane moving crack in a functionally graded piezoelectric layer between two dissimilar piezoelectric strips. J. Mech. Sci. Technol. Vol. 26, pp. 1017~1025

(13) Li, Y.D., Jia, B., Zhang, N., Tang, L. Q. and Dai, Y., 2006, Dynamic stress intensity factor of the weak/micro-discontinuous interface crack of a FGM coating, Int. J. Solids Strut. Vol. 43, pp. 4795~4809.

(14) Erdogan, F., 1985, The crack problem for bonded nonhomogeneous materials under antiplane shear loading, ASME J. Appl. Mech. Vol. 52, pp. 823~828.

(15) Pak, Y.E., 1990, Crack extension force in a piezoelectric materials, ASME J. Appl. Mech. Vol. 57, pp. 647~653.

(16) Narita, F., Shindo, Y. and Watanabe, K., 1999, Anti-plane shear crack in a piezoelectric layer bonded to dissimilar half spaces, JSME Int. J. Ser. A. Vol. 42, pp. 66~72.

(17) Jin, Z.H. and Batra, R.C., 1996, Some basic fracture mechanics concepts in functionally graded materials, J. Mech. Phys. Solids. Vol. 44, pp. 1221~1235.

(18) Wang, X.Y. and Yu, S.W., 2000, Transient response of a crack in piezoelectric strip subjected to the mechanical and electrical impact: mode III problem, Int. J. Solids Strut. Vol. 37, pp. 5795~5808.

(19) Kwon, S.M., Son, M.S. and Lee, K.Y., 2002, Transient behavior in a cracked piezoelectric layered composite: anti-plane problem, Mech. Mater. Vol. 34, pp. 593~603.

(20) Feng, W.J. and Su, R.K.L., 2006, Dynamic internal crack problem of a functionally graded magneto-electro-elastic strip, Int. J. Solids Strut. Vol. 43, pp. 5196~5216.